A New Four-Port Automatic Network Analyzer: Part I—Description and Performance

KJELL BRANTERVIK AND ERIK L. KOLLBERG, SENIOR MEMBER, IEEE

Abstract—A four-port automatic network analyzer based upon a new concept has been tested in the 8–12-GHz range. An essential feature of this analyzer, compared with the six-port systems, is that only one detector is used, and one electronically adjustable reference load is added. In this paper, an electronically adjustable short circuit is used as the reference load. Hence, the analyzer is comparatively simple and compact since only a few components are required. Moreover, the quality of the components can be moderate. A small desk-top computer (HP 85) is satisfactory for handling measurement data, adjusting the short circuit, and presenting the result.

A simplified theory required for the calibration and measurement procedure for the determination of the magnitude and the phase of an unknown load is included in this report, and experiments illustrate how the accuracy is improved when the calibration is gradially refined. The expected accuracy of the network analyzer is discussed in some detail.

The simple design and the moderate demands on the component quality means that it should be ideal for millimeter-wave frequencies.

I. Introduction

A NETWORK ANALYZER is an indispensable tool for testing microwave components and systems by measuring their complex scattering coefficients (phase and magnitude). In conventional automatic network analyzers, the magnitude as well as the phase are measured by equipment based on analog techniques [1]. Such analyzers include frequency converters, local oscillators, and phase detectors. Because of this relatively complicated design, conventional analyzers are quite expensive and have a limited measurement accuracy, particularly at higher frequencies (millimeter-wave range) [2]. It is therefore expected that the present design will have its main applications at millimeter-wave frequencies.

The six-port theory presented since 1972 involved a new approach in measuring complex scattering coefficients [3]–[7]. The hardware part was considerably simplified as compared with conventional analyzers. The automatic network analyzer discussed in this paper [8] represents a further step in the total system simplification. In this new analyzer, as well as in the six-port system, a small computer is an absolute necessity for evaluating the measured information.

Manuscript received June 20, 1984; revised February 11, 1985. This work was supported in part by the Swedish Board for Technical Development.

K. Brantervik is with the Department of Physics, Chalmers University of Technology, S-412 96 Göteborg, Sweden.

E. Kollberg is with the Department of Electron Physics 1, Chalmers University of Technology, S-412 96 Göteborg, Sweden.

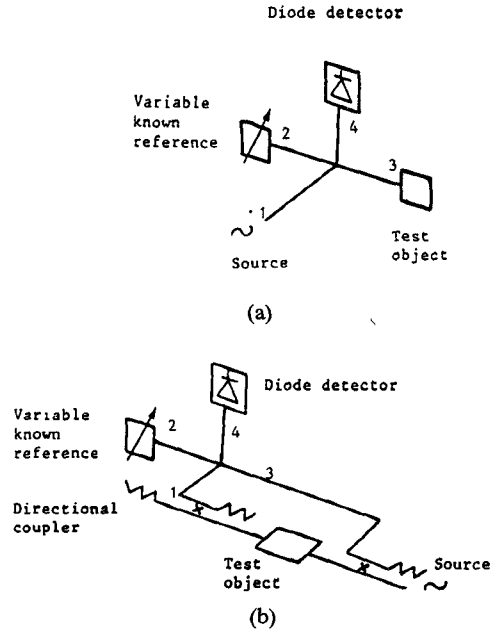

Fig. 1. Measurement setup for (a) reflection measurements and (b) transmission measurements.

II. Short Description of the Method

An arrangement for reflection measurements is shown in Fig. 1(a). Signal power is fed to port 1. In an arrangement for transmission measurements (Fig. 1(b)), two directional couplers are added. Part of the signal is fed to port 3 and another part transmitted through the test object and brought to port 1. For each frequency, at least three different values of the reference load (port 2) are needed for an unambiguous result in both arrangements (Fig. 1(a) and (b)).

For each state of the reference load, the power detected in port 4 is recorded. Each such measurement defines a circle in the complex scattering parameter plane (see Fig. 2). The common intersection point of the three circles represents the scattering parameter to be determined (the arrow in Fig. 2).

III. Basic Theory

Referring to Fig. 3, a_k represents the complex amplitudes of waves traveling towards the four-port, while b_k represents the complex amplitudes of waves traveling away

0018-9480/85/0700-0563$01.00 ©1985 IEEE

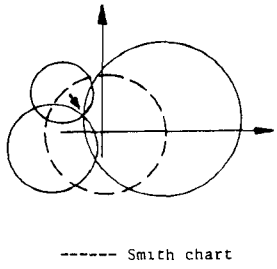

Fig. 2. Circles in the complex scattering parameter plane, defining possible values for the reflection (transmission) coefficient of the test object. The reference loads in this case are short circuits at different positions in the waveguide.

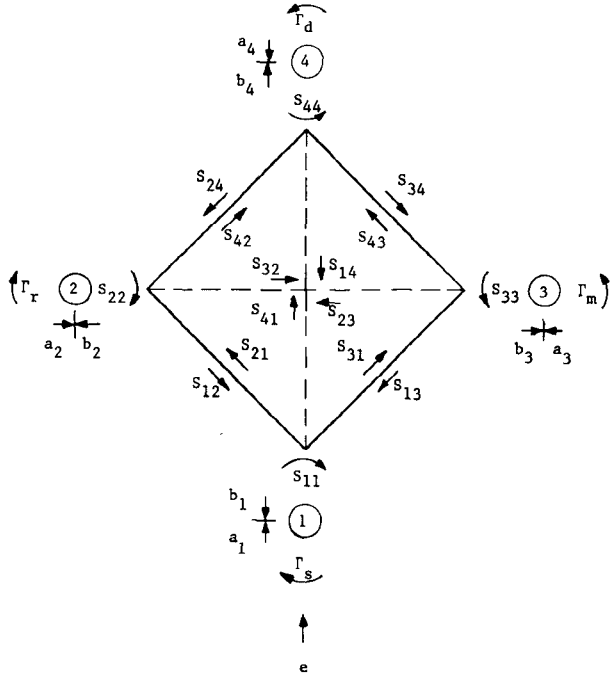

Fig. 3. Amplitudes and coefficients summarized.

from the four-port. S_{kl} are internal reflection and transmission coefficients. The indexes s, r, m, and d of the reflection coefficients Γ, indicate source, reference, measurement test object, and detector.

Let e represent the incoming wave amplitude from the generator. For a fixed frequency, e is a constant. The relation between the wave amplitudes a_1 and e is

$$a_1 = e + \Gamma_s \cdot b_1. \tag{1}$$

We also have

$$\left.\begin{aligned} b_1 &= S_{11}a_1 + S_{12}\Gamma_r b_2 + S_{13}\Gamma_m b_3 + S_{14}\Gamma_d b_4 \\ b_2 &= S_{21}a_1 + S_{22}\Gamma_r b_2 + S_{23}\Gamma_m b_3 + S_{24}\Gamma_d b_4 \\ b_3 &= S_{31}a_1 + S_{32}\Gamma_r b_2 + S_{33}\Gamma_m b_3 + S_{34}\Gamma_d b_4 \\ b_4 &= S_{41}a_1 + S_{42}\Gamma_r b_2 + S_{43}\Gamma_m b_3 + S_{44}\Gamma_d b_4 \end{aligned}\right\}. \tag{2}$$

Solving for b_4 (see the companion paper [9] or [10]), we obtain

$$b_4 = \frac{K_1\Gamma_m\Gamma_r + K_2\Gamma_r + K_3\Gamma_m + K_4}{K_5\Gamma_m\Gamma_r + K_6\Gamma_r + K_7\Gamma_m + 1}. \tag{3}$$

K_k in (3) can be expressed in terms of S_{kl}, Γ_d, and Γ_s (notice that $K_1 \cdots K_4$ are proportional to e). However, since they will be determined through a calibration procedure directly, there is no need here to show how they relate to the scattering parameters.

As mentioned above, the amplitude $|b_4|$ is measured for each adjustment of the reference load. For a specific adjustment, the relation between $|b_4|$ and Γ_m becomes

$$|b_4| = \left|\frac{A\Gamma_m + B}{C\Gamma_m + D}\right| \tag{4}$$

where A, B, C, and D are functions of Γ_r and K_k as realized when comparing (4) with (3). Equation (4) defines a circle with center location $(\Gamma_m)_{\text{center}}$ and radius $(\Gamma_m)_{\text{radius}}$ according to

$$(\Gamma_m)_{\text{center}} = \frac{\overline{\left(\frac{C}{D}\right)} \cdot \left|\frac{D}{A}\right|^2 \cdot |b_4|^2 - \frac{B}{A}}{1 - \left|\frac{C}{A}\right|^2 \cdot |b_4|^2} \tag{5}$$

$$(\Gamma_m)_{\text{radius}} = \frac{\frac{1}{|A|} \cdot \left|D - \frac{BC}{A}\right| \cdot |b_4|}{1 - \left|\frac{C}{A}\right|^2 \cdot |b_4|^2} \tag{6}$$

where

$$A = K_1\Gamma_r + K_3 \quad B = K_2\Gamma_r + K_4$$
$$C = K_5\Gamma_r + K_7 \quad D = K_6\Gamma_r + 1.$$

As mentioned above, $K_1 \cdots K_7$ are determined in a calibration procedure. Hence, $A \cdots D$ have to be calculated for each setting of the reference load.

The common intersection point of three circles (see Fig. 2) defines the correct complex value for Γ_m. However, usually the three circles do not intersect exactly in one point (compare Fig. 10 in the Appendix). It has been suggested [11] in this case to use the so-called "radical center" as the value for Γ (see Appendix).

For transmission measurements, an expression similar to (3) is obtained (see [9, eq. (15)]. Hence, the transmission coefficient can also be determined by searching for the common intersection point of three circles.

The methods described above will be referred to as the circle methods. There is, however, an even more accurate method, based on integration of the detector response over one-half waveguide wavelength [10]. We will not discuss this method further in this paper.

IV. System Description

A diagram of the automatic measuring system used in our experiments is shown in Fig. 4. The system is controlled by a small desk-top computer (HP 85) which performs all the required computations and interacts with the external devices through an HP-IB interface bus. The sweep oscillator, under computer control, supplies a 1-kHz square-wave modulated signal at selected frequencies.

In this paper, we discuss use of a movable short circuit as the reference load, i.e., we assume $\Gamma_r = e^{j\alpha}$ (α variable).

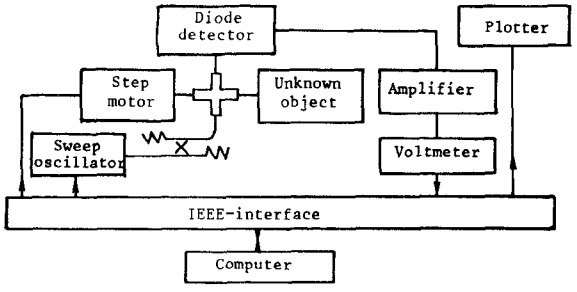

Fig. 4. Schematic diagram of the automatic measuring system.

At each selected frequency, the step motor adjusts the movable short circuit to three or more locations. The power at port 4 is registered by a square-law diode detector and the detected signal is amplified and fed to the digital voltmeter. The complex values of Γ_m are presented as functions of frequency on a plotter.

V. Simplified Calibration Procedure for Reflection Measurements

In order to illustrate the importance of an accurate and complete calibration, a simplified calibration method will be used and the magic T will be assumed perfectly symmetric. For a system intended for more precise measurements, the more involved and exact calibration methods described in [9] and [10] is recommended.

Three procedures are used, utilizing a matched load and a movable computer-controlled short circuit as terminations of ports 2 and 3.

A. Port 2: Movable short circuit, $\Gamma_r = 1 \cdot e^{j\alpha}$
Port 3: Matched load, $\Gamma_m = 0$

B. Port 2: Matched load, $\Gamma_r = 0$
Port 3: Movable short circuit, $\Gamma_m = 1 \cdot e^{j\alpha}$

C. Ports 2 and 3: Movable short circuit, $\Gamma_r = 1 \cdot e^{j\alpha}$, $\Gamma_m = 1 \cdot e^{j\beta}$.

In procedure A, the movable short circuit is adjusted over at least one wavelength. Inserting $\Gamma_r = e^{j\alpha}$ and $\Gamma_m = 0$ into (3), we obtain for procedure A

$$\frac{1}{|b_4|} = \frac{|1 + K_6 e^{j\alpha}|}{|K_2| \cdot \left|1 + \frac{K_4}{K_2} e^{-j\alpha}\right|}. \tag{7}$$

In a perfectly symmetric magic T, we have $S_{41} = 0$, $S_{42} = -S_{43}$, $S_{12} = S_{13}$, $(S_{ij} = S_{ji})$. From [9, eq. (11b)], this yields $K_1 = 0$ and $K_4 = 0$. Equation (7) results in a variation of $1/|b_4|$ as shown in Fig. 5. From this pattern, $|K_2|$, $|K_6|$, and Φ_6 can be determined assuming $K_4 = 0$. The argument Φ_6 of K_6 is

$$\Phi_6 = \pi/2 - \alpha_1 \text{ or } \Phi_6 = 3\pi/2 - \alpha_2. \tag{8}$$

Procedure B yields $|K_7|$, Φ_7, and $|K_3|$ in exactly the same way as discussed for procedure A. For a perfectly symmetric magic T, $K_6 = K_7$ and $K_2 = -K_3$. This result is reasonable in view of (3). For a detailed evaluation, the equations in [9, eqs. (9)–(11)] have to be considered. We

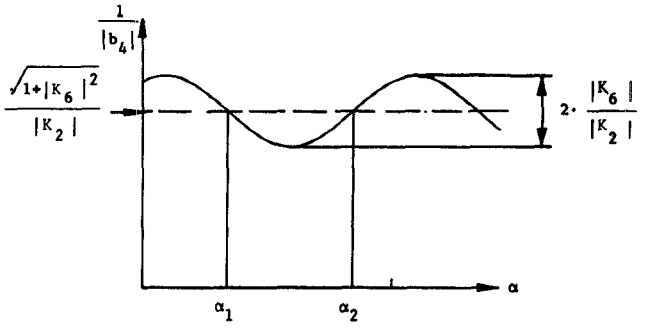

Fig. 5. Calibration measurement by one short circuit and one termination.

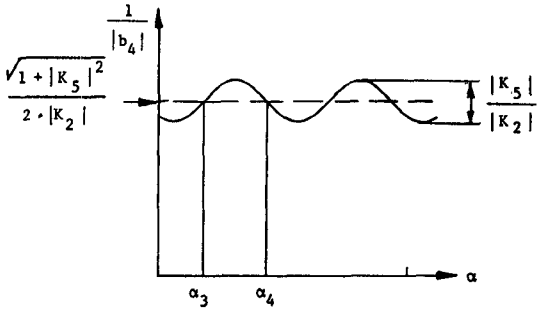

Fig. 6. Calibration measurement by two short circuits with a phase difference π.

therefore will use the mean value ($|K_6| = |K_7| = (|K_6| + |K_7|)_{meas}/2$, etc.) for the measurements described in the next section. With $\Gamma_m = e^{j\alpha}$, $\Gamma_r = e^{j\beta}$, $K_7 = K_6$, $K_3 = -K_2$, $K_4 = 0$, and $K_1 = 0$ inserted in (3), we obtain

$$\frac{1}{|b_4|} = \frac{|K_5 e^{j(\alpha+\beta)} + K_6(e^{j\alpha} + e^{j\beta}) + 1|}{|K_2| \cdot |e^{j\alpha} - e^{j\beta})|}. \tag{9}$$

With the short-circuit plane adjusted so that $\beta = \alpha + \pi$, a variation of $1/|b_4|$ versus α (as shown in Fig. 6) is obtained. Hence, $|K_5|$, Φ_5, and $|K_2|$ can be determined, where

$$\Phi_5 = \frac{\pi}{2} - 2\alpha_3 \text{ or } \Phi_5 = \frac{3\pi}{2} - 2\alpha_4.$$

VI. Measurements Using the Simplified Calibration Procedure

Having performed the calibration steps described in Section V, preliminary measurements were made. The parameters K_2, K_3, K_5, K_6, and K_7 are known for the calibration program, but the parameters K_1 and K_4 are assumed negligable. In addition, the phase of Γ_r is determined only from knowledge of the physical location of the movable short circuit, both in the calibration processes of Section III and in the preliminary measurements described in this section.

Fig. 7 shows the results obtained using as a test object a movable short circuit, similar to the one used as the reference. The different results obtained when the reference and measurement object change positions, indicate the error introduced due to existing asymmetries. This is further illustrated by taking the mean of the two measurements, yielding a much smaller error. The elimination of

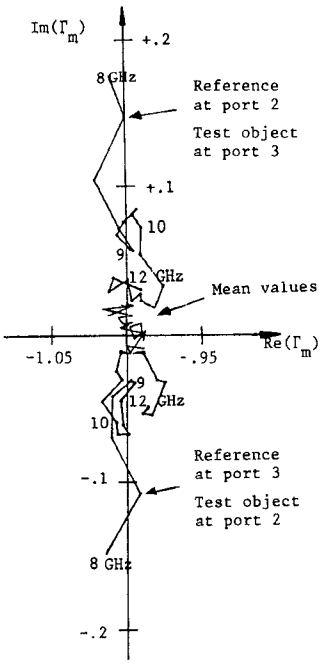

Fig. 7. Measurements on a short circuit similar to the one used as a reference load, and at a reference position where one expects $\Gamma = -1 + j0$ independent of frequency. The upper and the lower curves show results obtained when the measured short circuit and the reference short circuit are interchanged. The mean value of these two measurements is also displaced.

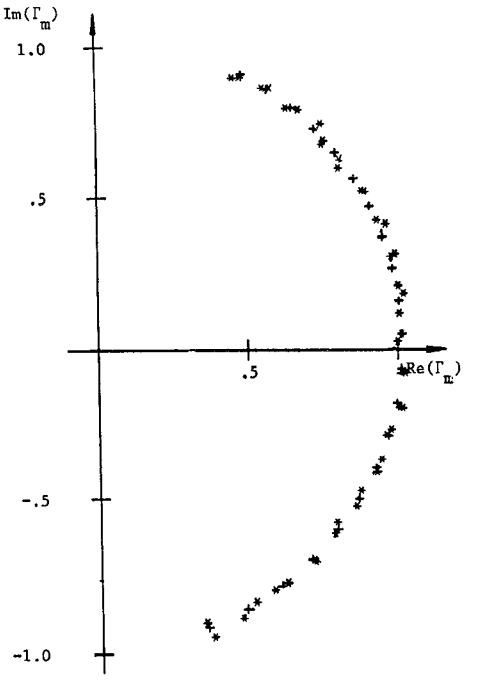

Fig. 8. Results from measurements with the short-circuit plane at a position $l_0 = 10$ mm away from the position used in Fig. 7 (reference position) expected to yield $\Gamma = -\exp(j2\pi \cdot l_0/\lambda_g)$. For further comments, see the text.

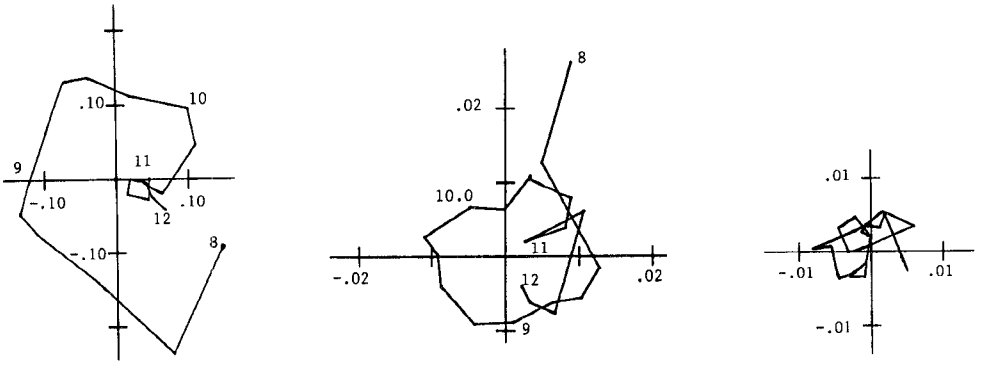

Fig. 9. Results from measurements on a matched load. (a) Parameter values of $K1, K4, K5, K6, K7$ neglected. (b) Parameter values of $K4$ neglected. (c) All the system parameters accounted for.

errors due to asymmetry can consequently be obtained in this way.

Fig. 8 shows the results obtained with the same test object as above, but with the short-circuit plane moved to a new position 10 mm closer to the magic T. Measurements, with the test object at port 2 and at port 3, respectively, have been represented in the same diagram. The "+" symbols denote the theoretical values. The errors in Fig. 8 are comparable with the errors in Fig. 7, which means errors of about 3 percent from each of the single series of measurements, and less than half as much if average values from the two series are taken.

In the measurements shown in Fig. 9, the test object is a matched load (HP, X914B). The improvement obtained with successively better knowledge of the system parameters is illustrated.

Notice that in all the measurements reported above, the phase is defined relative to the position of the movable short circuit. In order to have a more exact knowledge of the phase, a polished metal plate should be used at the test port. In the companion paper [9], the precision calibration procedure described also involves use of such a polished plate. This calibration procedure also very accurately gives the phase and amplitude of all seven system parameters $(K_1 \cdots K_7)$.

VII. Measurement Accuracy

In this section, we will investigate the obtainable accuracy when the complete precision calibration procedure described in [9] is used. The discussion below is based on the experience obtained from experiments, some of them

reported in this paper. The precision calibration method as such has been checked experimentally with a semi-automatic measurement system at one frequency. However, extensive tests have subsequently been performed by computer simulations. By assuming a certain set of system parameters, the detected signal was calculated for two known and variable reference coefficients Γ_2 and Γ_3. Then, this calculated signal was used for evaluating the system parameters. Also, errors in the detected power measurement have been simulated. The system parameters obtained in the calibration procedures are compared with those used for the signal calculation. The results are presented below for four different measurement cases. The experimental measurements reported above support the validity of such simulations.

Due to the integration procedure used during the calibration, errors depending on irregularities in the reference load adjustment, as well as errors depending on detector noise, are almost eliminated. Departures from detector linearity influence the accuracy in determining the scattering coefficient of a test object in two different ways. First, the accuracies of the system parameter determination depend on the detector linearity. Second, the registered power values during the test object measurements also depend on the detector linearity. Hence, the accuracy in determining the scattering parameters of the test object depend on both the accuracy of the system parameters and the accuracy in the registered powers.

The error, depending on system parameter inaccuracies, can roughly be estimated from the computer simulations as within twice the relative departure from linearity of the detector if the circle method is used, while for the integration method (see [10]) the associated error is a factor of two smaller.

However, besides errors caused by the detector, additional contributions have to be considered. These additional errors depend on both the measurement arrangement and the method used. A review of some methods and arrangements are given below:

a) reflection measurements, circle method (this paper),
b) reflection measurements, integral method [10],
c) transmission measurements, circle method.

For the measurement cases above, all the internal scatterings in the measurement arrangement can be compensated for, with one exception. For case c), the accuracy is limited by possible multiple scatterings in the directional coupler, which links the test object and the four-port (see Fig. 1 (b)).

Dimensional errors of waveguides, etc., in the analyzer will not be important due to the nature of the calibration procedure. However, temperature effects may have to be considered if measurements are performed at temperatures considerably different from those used at the calibration. The compact construction of the analyzer should make such temperature effects comparatively small.

With dimensional errors and leakage kept under control, the different main error contributions will be indicated as follows:

δx relative detector noise and (systematic) irregularities in the used reference load (estimated),
δy relative error in detector linearity including the diode as well as the amplifier (estimated),
δs errors due to system parameter inaccuracies (estimated from computer simulations); $\delta s = \delta y$ for case b) and $\delta s = 2\delta y$ for cases a), c), and d),
δz average primary line reflection coefficient of the directional coupler, which links the test object and the four-port (only case c) above). In the error budget, δz^2 should be multiplied by $|S_{22}|^2$. We will use $|S_{22}|^2 = 0.25$.

Hence, the systematic error in magnitude

$$\left(\sqrt{\delta s^2 + \delta x^2 + \delta y^2 + 0.25 \cdot \delta z^2}\right)$$

and in phase

$$\left(60 \cdot \sqrt{\delta s^2 + \delta x^2 + \delta y^2 + 0.25 \cdot \delta z^2}\right) Q$$

becomes

$$\left.\begin{aligned} &\text{Magnitude} = \sqrt{\delta x^2 + 5\delta y^2} \\ &\text{Phase degrees} = 60\sqrt{\delta x^2 + 5\delta y^2}\,/Q \end{aligned}\right\} \quad \text{Case a)}$$

$$\left.\begin{aligned} &\text{Magnitude} = \sqrt{2}\,\delta y \\ &\text{Phase degrees} = 100\,\delta y/Q \end{aligned}\right\} \quad \text{Case b)}$$

$$\left.\begin{aligned} &\text{Magnitude} = \sqrt{\delta x^2 + 5\delta y^2 + 0.25\delta z^2} \\ &\text{Phase degrees} = 60\sqrt{\delta x^2 + 5\delta y^2 + 0.25\delta z^2}\,/Q \end{aligned}\right\} \quad \text{Case c)}$$

Errors due to a finite directivity of the input directional coupler is not included in the formula yielding case c). The notation Q above is equal to the magnitudes of the measured reflection or transmission coefficients, respectively.

However, the systematic errors are somewhat smaller for small measured reflection and transmission magnitudes ($Q < 1$) than the expressions above indicate. A rough estimation leads to the following magnitudes for δx, δy, and δz for frequencies up to 100 GHz:

$\delta x = 0.0002$–0.001
$\delta y = 0.0002$–0.0005 (for diode detectors)
$\delta z = 0.01$–0.04.

The estimations of δx and δy above have been obtained considering use of low-noise chopper amplifiers and a dynamic range between 30 and 40 dB. Errors due to the amplifier and detector linearity are discussed extensively in [12]. With these values inserted in the error functions above, the total systematic errors for $Q \leqslant 1$ can be estimated as follows:

Case	Magnitude	Phase, degrees
a), b)	0.0005–0.002	$0.02/Q$–$0.1/Q$
c)	0.005–0.02	$0.2/Q$–$1/Q$

Error contributions depending on possible inaccuracies in the frequency adjustments are not included in the esti-

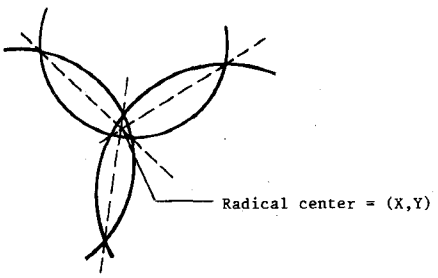

Fig. 10. The common chords of three circles intersect in a point (X, Y) known as the radical center.

mations above. Although extensive systematic measurements have to be performed to get more detailed information about what accuracy can be achieved for different frequency ranges, it should be possible to achieve an accuracy comparable to the accuracy of a six-port system.

Although the accuracy estimation in this section is based on experience with a movable short circuit, nearly the same accuracy should be obtainable using, for example, a varactor diode as a reference load. However, the system has to be calibrated as described in the companion paper [9]. The scattering properties of the varactor diode has to be determined separately, using a movable short circuit as the reference.

Appendix

If the center of the ith circle is (x_i, y_i) and the radius of the ith circle is r_i, then the relevant intersection point (x, y) of the three circles can be calculated as "the radical center" [10] of these circles (see Fig. 10).

$$(X,Y)=\left(\frac{\begin{vmatrix} R & R' \\ Q & Q' \end{vmatrix}}{\begin{vmatrix} P & P' \\ Q & Q' \end{vmatrix}},-\frac{\begin{vmatrix} R & R' \\ P & P' \end{vmatrix}}{\begin{vmatrix} P & P' \\ Q & Q' \end{vmatrix}}\right) \tag{A1}$$

where

$$P=2(x_2-x_1)$$
$$P'=2(x_3-x_1)$$
$$Q=2(y_2-y_1)$$
$$Q'=2(y_3-y_1)$$
$$R=r_1^2-r_2^2+x_2^2-x_1^2+y_2^2-y_1^2$$
$$R'=r_1^2-r_3^2+x_3^2-x_1^2+y_3^2-y_1^2.$$

Acknowledgment

The authors would like to acknowledge Dr. C. Hagström for his help in the initial phase of the project and Prof. O. Nilsson for fruitful discussions. They would also like to thank G. Aspevik for typing the manuscript.

References

[1] "Network analysis at microwave frequencies," HP Application Note 92.

[2] A. P. Jeffrey, "Wideband millimeter-wave impedance measurements," *Microwave J.*, vol. 26, no. 4, pp. 95–102, 1983.

[3] C. A. Hoer, "The six-port coupler: A new approach to measuring voltage, current, power, impedance, and phase," *IEEE Trans. Instrum. Meas.*, vol. IM-21, pp. 466–470, Nov. 1972.

[4] G. F. Engen and C. A. Hoer, "Application of an arbitrary six-port junction to power measurement problems," *IEEE Trans. Instrum. Meas.*, vol. IM-21, pp. 470–474, Nov. 1972.

[5] G. F. Engen, "Determination of microwave phase and amplitude from power measurements," *IEEE Trans. Instrum Meas.*, vol. IM-25, pp. 414–418, Dec. 1976.

[6] G. F. Engen, "The six-port reflectometer: An alternative network analyzer," *IEEE Trans. Microwave Theory Tech.*, pp. 1075–1079, Dec. 1977.

[7] J. R. Juroshek and C. A. Hoer, "A dual six-port network analyzer using diode detectors," *IEEE Trans. Microwave Theory Tech.*, pp. 78–82, Jan. 1984.

[8] C. Hagström and E. Kollberg, Swedish Patent 82-04801-8, U.S. Patent pending.

[9] K. Brantervik, "A new four-port automatic network analyzer: Theory," *IEEE Trans. Microwave Theory Tech.*, this issue.

[10] K. Brantervik, "Improved calibration methods for the variable reference network analyzer," Applied Electron Physics, Chalmers Univ. of Technology, Göteborg, Sweden, Rep. No. 3, 1984.

[11] G. F. Engen, "A least squares solution for use in the six-port measurement technique," *IEEE Trans. Microwave Theory Tech.*, vol. MTT-28, pp. 1473–1477, Dec. 1980.

[12] C. A. Hoer, K. C. Roe, and C. M. Allred, "Measuring and minimizing diode detector nonlinearity," *IEEE Trans. Instrum. Meas.*, vol. IM-25, Dec. 1976.

Kjell Brantervik was born in Kristianstad, Sweden, on August 15, 1941. From 1961 to 1966, he worked as an aerotechnical engineer at Saab in Linköping. In 1968, he received the M.Sc. degree in mathematics and physics and worked as a high-school teacher in these subjects from 1968 to 1978. He received the M.Sc. degree in technical physics at the University of Technology in Lund in 1976. From 1979 to 1984, he worked as a Research Engineer at the Department of Applied Electron Physics at Chalmers University of Technology in Göteborg. During this period, he worked on a new type of network analyzer for microwaves and millimeter-waves. He received the D.Sc. in electrical engineering in 1984. Since 1984, he has been working on nonlinear electric phenomena in thin films at the Department of Physics at Chalmers University of Technology in Göteborg.

Erik L. Kollberg (M'83–SM'83) was born in Stockholm, Sweden. He received the M.Sc. degree in electrical engineering in 1961, the Tekn. Licentiat degree in 1965, and the Teknologie Doktor degree in 1970, all from Chalmers University of Technology, Göteborg, Sweden.

He is now a Professor at Chalmers University of Technology and is responsible for development of low-noise receivers for the Onsala Space Observatory. From 1963 to 1976, he worked on low-noise maser amplifiers. He has developed eight masers for the Onsala Space Observatory, ranging in frequency from 1 to 36 GHz. Since 1972, he has also been working on low-noise millimeter-wave mixers. These mixers have been used for radio astronomy observations at Onsala since 1979. More recently, he has been working on extremely low-noise superconducting (quasi-particle) mixers, and experimental receivers are now in use at the Onsala Observatory. He and his coworkers have also started development work on GaAs millimeter-wave components. In the fields mentioned above, he has authored about 60 scientific papers and edited one book, *Microwave and Millimeter-Wave Mixers* (IEEE Press). At the 1982 12th European Microwave Conference in Helsinki, he and his coauthors were awarded the Microwave Prize. Aside from his research and development work, he also lectures at the University.

Dr. Kollberg is Chairman of the Microwave Theory and Techniques Chapter of the IEEE Swedish Section. He is also a member of the Swedish branch of URSI.